International Journal of Environmental Impacts
https://www.acadlore.com/journals/IJEI

Predicting Water Availability in the Chalcas River Basin: Application of Artificial Neural Networks for Sustainable Resource Management

Hemerson Lizarbe-Alarcón*, Jhac Taboada-Valenzuela, Edward León-Palacios, José Estrada-Cardenas, Rocky Ayala-Bizarro, Main Tenorio-Palomino, Rualth Bravo-Anaya, Alex Ircañaupa

Management, Construction and Transportation Studies–GECOTRAN, Universidad Nacional de San Cristobal de Huamanga, 05001 Ayacucho, Peru

* Correspondence: Hemerson Lizarbe-Alarcón (hemerson.lizarbe@unsch.edu.pe)

Received: 10-06-2025 **Revised:** 11-07-2025 **Accepted:** 11-24-2025

Citation: H. Lizarbe-Alarcón, J. Taboada-Valenzuela, E. León-Palacios, J. Estrada-Cardenas, R. Ayala-Bizarro, M. Tenorio-Palomino, R. Bravo-Anaya, and A. Ircañaupa, "Predicting water availability in the Chalcas River basin: Application of artificial neural networks for sustainable resource management," *Int. J. Environ. Impacts.*, vol. 9, no. 2, pp. 445–455, 2026. https://doi.org/10.56578/ijei090210.

Abstract: This study aimed to develop a predictive model of water availability using artificial neural networks (ANN) in the Chalcas River basin, located in the district of San Pedro de Palco, Ayacucho, Peru. A quantitative, predictive, and non-experimental longitudinal design was applied. Hydrological data were used, including monthly average precipitation (ranging from 3.44 mm in June to 123.49 mm in February), weighted crop coefficients (Kc), monthly evapotranspiration (ETo), and a drainage density of 5.81 km/km^2. A multilayer ANN was structured and trained over 2000 epochs, achieving an average accuracy of 90.62% and a normalized mean absolute error (MAE) of 0.0528. The model determined the flow rate for the period 2003–2030 period, identifying critical seasonal patterns: a peak of 317.45 l/s in January 2028 and a minimum of 28.55 l/s in July 2026. These findings highlight the need to implement water storage strategies during wet seasons and optimize water use during dry periods. Ultimately, the ANN-based model enhances water resource management, reduces scarcity-related risks, and promotes the sustainability of the irrigation system. This methodology demonstrates broad applicability and can be replicated in other basins facing similar hydrological challenges, using the ANN model.

Keywords: Artificial neural networks; Hydrological modeling; Multilayer Perceptron; Risk management; Water management

1 Introduction

Water resources are a vital component for sustaining life, development, and the sustainability of ecosystems [1]. Understanding this relationship requires analyzing climatic, topographic, and anthropogenic factors that influence water behavior within a watershed.

A fundamental tool for estimating water availability is the water balance, which quantifies the parameters involved in the hydrological cycle [2], including system inputs and outputs through the analysis of variables such as precipitation, evapotranspiration (ETo), streamflow, and storage [3]. However, accurate estimation depends on rigorous processing of available hydrometeorological data, which must undergo validation processes such as consistency analysis, double mass curve, linear regression, and other statistical methods [4].

Watersheds, as the basic units of hydrological analysis, are influenced by the topographic characteristics of the environment, which affect their hydrometeorological processes and resource utilization [3]. Additionally, physiographic and climatic characteristics of the basin—such as stream order, drainage network length, and slope—are essential for building hydrographs, understanding surface flow dynamics, analyzing rainfall–runoff relationships, and predicting the hydrological behavior of the basin [5].

In regions like the Chalcas River basin, located in the district of San Pedro de Palco, Ayacucho, Peru, water availability and efficient management represent critical challenges. High climatic variability and complex geographical conditions significantly affect water resources, making streamflow prediction difficult and limiting timely planning for rational water use [6]. This basin faces significant water constraints attributable to rainfall seasonality, limited monitoring infrastructure, and the absence of predictive management systems. These conditions have reduced local agricultural yields to less than 70% of their potential. In this context, river flow prediction becomes crucial, as it allows anticipation of available water for various activities and supports informed decision-making regarding resource use [6].

Traditionally, hydrological behavior in watersheds has been simulated using deterministic hydrological models such as Hydrological Engineering Centre's Hydrological Modeling System (HEC-HMS), Soil and Water Assessment Tool (SWAT), or Sacramento Soil Moisture Accounting (SAC-SMA) [7]. However, these models often require extensive calibration and frequently fail to adequately capture the nonlinear nature of hydrological systems [7]. In response to these limitations, artificial neural network (ANN)-based models have emerged strongly, demonstrating superior capacity to identify complex relationships among multiple variables and estimate streamflow even with incomplete data or high variability [8].

ANNs have proven particularly effective in modeling complex nonlinear systems such as hydrological processes [6]. Their ability to capture nonlinear relationships between meteorological and hydrological variables makes them key tools in water resource management and disaster prevention [9]. Among the most effective architectures is the Multilayer Perceptron (MLP), a feedforward neural network that applies a weighted sum of inputs followed by a nonlinear activation function, and is trained using the backpropagation algorithm [10]. This training process adjusts synaptic weights to minimize error, allowing the model to efficiently learn hydrological behavior patterns [11].

This potential has been validated in numerous studies comparing the performance of ANN models, including the following research: ANN in deep learning for prediction substantially improve the learning of concepts and procedures [12], the integration of the ANN approach with the HEC-RAS model has improved prediction accuracy compared to traditional methods [13], a comparison between ANNs and the hydrological model using the HEC-HMS concluded that the ANN algorithm proved superior among data-based models in the context of simulations and can be used to simulate river flow with an acceptable level [14], the simulation results indicate that the runoff simulated by the ANN was closer to the observed values than that predicted by the Hydrological Simulation in Fortran (HSPF) model [15], ANN models can be superior to conventional conceptual-type models of Precipitation-runoff [16]. SWAT and ANN models were evaluated and compared. SWAT proved more effective at simulating low flows, while ANNs were superior in estimating high flows in all cases. [17]. Identification of Hydrographs And Components from Rainfall, Evaporation and Streamflow (IHACRES), a physically based hydrological model, and ANNs were used to simulate daily flow. The ANN model proved to be a viable alternative for complex hydrological systems with poor recorded data [18]. For example, studies conducted in Peruvian basins have applied Long Short-Term Memory (LSTM) models using precipitation and flow records, obtaining Nash-Sutcliffe coefficients greater than 0.90 during the validation phase [19]. Other recent comparative results highlight the superiority of ANN models in predicting extreme events such as floods and droughts [20], which has driven their increasing use in regions with limited reliable data and high climate variability.

The model was designed not only to anticipate monthly water availability in the basin but also to evaluate its impact on water management and irrigation system efficiency. To achieve this, an MLP neural network was designed, trained, and validated using historical hydrometeorological data from the basin, with the goal of generating projections for the 2003–2028 period. Model development involved statistical data processing, morphometric analysis of the basin, and the integration of the conceptual Lutz–Scholz hydrological model as a basis for defining input variables. Programming tools such as Python and MATLAB were used to implement the model, using key variables such as monthly precipitation, reference ETo, weighted crop coefficients (Kc), and historical average streamflows. The model was evaluated using performance metrics such as accuracy, normalized mean absolute error (MAE), and seasonal trend analysis.

The results obtained not only identified critical periods of water scarcity and abundance but also provided a solid foundation for improving irrigation management and agricultural planning in the region. Additionally, this approach can be adapted to other basins with similar characteristics, contributing to the strengthening of regional water security strategies in the face of climate change effects.

2 Materials and Methodology

The study was conducted in the Chalcas River basin, located in the district of San Pedro de Palco, Ayacucho region, Peru. This region exhibits a marked climatic seasonality, characterized by periods of intense rainfall followed by prolonged dry seasons, which significantly affect water resource availability. The geographic location and main coordinates of the basin are presented in Table 1.

Table 1. Location of the Chalcas River basin

Basin Name	North Capture Point (m)	East Capture Point (m)	Elevation (masl)	Basin Area (km^2)	Basin Perimeter (km)
Chalcas River	8,409,506.00	535,900.00	2,641.10	164.41	67.73

A quantitative approach with a predictive scope was applied, aimed at modeling water availability using advanced forecasting techniques. The methodological design was non-experimental, longitudinal, and panel-type, since it used historical records of hydrometeorological variables collected continuously over an extended period.

The study population consisted of historical records of precipitation, temperature, and streamflow corresponding to the Chalcas River basin, in the district of San Pedro de Palco, Ayacucho region. The data were obtained from the Lucanas and Puquio meteorological stations and the Chalcas hydrological station, all registered by the National Meteorology and Hydrology Service of Peru (SENAMHI). The sample consisted of monthly data from 1980 to 2002, selected through non-probabilistic convenience sampling due to the continuous and high-quality availability of information during that interval.

The main research hypothesis was as follows: the predictive model based on ANN enables highly accurate estimation of water availability in the Chalcas River basin, district of San Pedro de Palco, Ayacucho.

The study variables were:

• Independent variable: Predictive model based on ANN.

Indicators:

Neural network architecture.

Number of hidden layers.

Number of neurons per layer.

Model accuracy.

Root Mean Square Error (RMSE).

• Dependent variable: Water availability.

Indicators:

Monthly average streamflow.

Projected volume.

Precipitation.

Percentage of efficient use of available water resources.

Monthly distribution of water resources.

The research employed techniques such as literature review to support the use of ANN in hydrological forecasting, and data collection from SENAMHI's meteorological and hydrological stations. Instruments included statistical software such as Python and its libraries (Pandas, NumPy, SciPy), visualization tools like Matplotlib, and data record sheets to organize the collected information. To analyze the data and validate the ANN model, various statistical techniques were applied, including time series decomposition, correlation analysis, and linear and nonlinear regression. The model's performance was evaluated using metrics such as mean squared error (MSE), RMSE, and the coefficient of determination (R^2).

The methodological procedure included several stages:

• Hydrometeorological analysis of historical precipitation, temperature, and streamflow series, considering records from stations located in the upper part of the basin of the Río Cachi special project. The meteorological stations selected for this analysis are described in Table 2.

Table 2. Meteorological stations with similar altitude and hydrometeorological characteristics to the project area

Meteorological Station	Type	Latitude (° ' ")	Longitude (° ' ")	Average Altitude (masl)	Region	Province	District
Lucanas	Conventional, Meteorological	14° 37' 00.00"	74° 13' 00.00"	3,354.00	Ayacucho	Lucanas	Lucanas
Puquio	Conventional, Meteorological	14° 41' 00.00"	74° 07' 00.00"	3,168.00	Ayacucho	Lucanas	Puquio
Paucocorral	Conventional, Meteorological	14° 40' 00.00"	74° 06' 00.00"	4,060.00	Ayacucho	Lucanas	Puquio
Huanca Sancos	Conventional, Meteorological	13° 55' 00.00"	74° 20' 00.00"	3,553.00	Ayacucho	Huanca Sancos	Sancos
Querobamba	Conventional, Meteorological	14° 01' 00.00"	73° 50' 00.00"	3,502.00	Ayacucho	Sucre	Querobamba
Paico	Conventional, Meteorological	14° 02' 00.00"	73° 40' 00.00"	3,589.00	Ayacucho	Sucre	Paico

• Evaluation of data consistency and quality using graphical techniques (double mass curve), statistical tests (Student's t and Fisher's F tests), and jump analysis.

• Analysis of the geomorphological parameters of the basin to determine the hydrological behavior and describe natural processes. The main morphometric results are presented in Table 3.

Table 3. Geomorphological characteristics of the Chalcas River basin

Description	Unit	Value
Basin area and perimeter		
Area	km^2	164.41
Perimeter	km	67.73
Elevations		
Maximum elevation	masl	4,400.00
Minimum elevation	masl	2,641.10
Centroid (WGS: 1984 UTM ZONE 18S)		
X centroid	km	537.52
Y centroid	km	8,417.94
Z centroid	masl	3,738.55
Altitude		
Mean altitude	masl	3,738.55
Most frequent altitude	masl	4,211.00
Mean frequency altitude	masl	4,193.00
Hydrographic network		
Main course length	km	23.39
Stream order	units	7.00
Stream network length	km	955.03
Average stream slope	%	1.52
Calculated parameters		
Horton's Form Factor (Kf)	–	0.30
Gravelius Compactness Index (Kc)	–	1.48
Miller's Circularity Coefficient (Cc)	–	0.45
Drainage Density (D)	km/km^2	5.81
Time of Concentration	hours	1.77

Table 4. Calculated monthly precipitation in the Chalcas River basin

Year	Jan	Feb	Mar	Apr	May	Jun	Jul	Aug	Sep	Oct	Nov	Dec	Total
1980	77.42	53.73	124.56	4.41	2.63	0.39	8.07	1.07	12.36	36.63	16.21	28.75	366.25
1981	93.32	207.52	135.6	45.74	5.6	1.3	1.23	24.35	9.6	7.72	23.42	94.74	549.72
1982	113.33	115.82	106.98	40.69	4.52	0.92	2.31	5.8	19.55	34.22	44.6	31.86	522.78
1983	75.09	80.2	98.73	33.55	3.08	1.32	1.08	2.19	13.78	17.91	15.8	53.43	397.05
1984	132.19	149.93	142.07	37.92	7.07	10.9	2.74	5.36	12.94	23.2	42.53	67.02	634.48
1985	86.25	166.44	292.17	68.57	24.06	11.19	1.71	4.26	8.06	14.21	24.47	77.18	794.56
1986	189.56	166.17	214.35	43.22	7.18	1.42	2.78	7.1	8.93	6.14	10.1	77.62	754.62
1987	149.01	91.27	93.04	35.4	5.59	3.79	0.91	1.49	11.03	19.1	25.82	44.74	561.19
1988	115.52	130.58	112.63	39.69	17.03	0.61	2.27	1.76	5.78	14.14	12.6	79.13	532.25
1989	240.09	185.16	186.39	37.08	8.39	2.29	1.89	6.04	3.07	14.81	20.15	41.09	746.45
1990	108.29	71.95	103.45	33.59	38	28.89	1.25	11.97	19.91	38.38	60.48	78.95	595.1
1991	85.07	68.19	165.25	32.55	9.34	3.28	1.27	1.98	5.53	14.25	18.67	22.1	426.27
1992	34.19	66.03	61.45	14.03	1.91	1.82	2.59	3	3.11	18.32	28.97	28.97	255.4
1993	115.58	123.83	109.05	47.2	10.14	0.82	2.34	7.73	12.67	24.55	35.57	65.12	555.67
1994	167.91	107.9	183.77	25.76	17.05	15.41	4.08	16.42	12.92	12.08	28.17	56.42	726.28
1995	109.95	89.83	168.61	25.13	1.55	0.71	1.04	1.48	11.49	14.85	57.02	59.6	546.17
1996	145.98	214.41	124.23	82.89	6.1	0.32	1.41	9.03	11.49	23.78	34.18	84.6	698.53
1997	125.23	140.59	87.69	35.99	8.24	0.31	2.05	20.68	16.91	16.91	37.21	98.33	689.53
1998	178.02	115.25	121.4	22.91	0.93	0.03	0.04	2.43	3	19.92	41.68	82.47	521.17
1999	122.33	202.2	133.23	44.31	10.57	1.12	4.5	0.77	20.94	45.33	20.88	75.51	681.69
2000	189.93	183.99	149.28	25.38	10.18	4.85	5.23	11.35	9.51	58.05	24.87	99.58	770.19
2001	160.37	138.35	182.82	52.5	18.89	2.5	7.01	10.08	11.32	17.37	34.91	42.31	678.24
2002	123.4	149.53	157.39	38.3	15.36	5.28	19.24	8.46	17.96	22.12	50.34	84.35	689.75
Data count							23						
Mean	107.7	123.49	108.17	39.17	8.74	3.44	7.91	7.31	11.91	22.11	24.05	31.44	141.64
Std. Dev.	45.79	51.34	48.95	13.79	8.61	6.72	3.94	6.29	5.5	12.22	14.14	14.64	141.64
Coef. Var.	0.36	0.38	0.35	0.48	0.85	1.42	0.48	0.86	0.48	0.55	0.47	0.38	0.24
Max. Prec.	240.09	214.41	292.17	88.57	38	28.89	19.24	24.38	20.94	56.05	100.46	99.58	798.56
Min. Prec.	34.19	53.73	61.45	4.41	0.93	0.31	0.64	0.77	3	6.14	10.1	22.1	255.4
75% Conf. range	89.89	107.72	107.72	23.7	4.37	0.94	0.78	3.09	7.67	13.92	20.41	49.02	400.36

Note: 1. Source: Technical Report No. 002-2020 ANA-AAA-CH.CH-ALA GRANDE – District Municipality of San Pedro de Palco, 2020 [21]. 2. Monthly precipitation was calculated using isohyets based on historical records from meteorological stations [22].

• Estimation of water supply using the Lutz-Scholz model, suitable for basins with limited records or variable conditions. The model used the complete monthly precipitation record for the Chalcas River basin, from January 1980 to December 2002, totaling 276 data points. These data were obtained from the meteorological stations of Lucanas, Sucre, and Huanca Sancos and served as input variables for building the ANN predictive model. This allowed for the generation of average monthly flows, reaching approximately 250 l/s during the wet season (January–March) and around 30 l/s in the dry season (June–August), which served as the basis for comparative analysis against water demand. Table 4 presents the complete monthly precipitation record for the 1980–2002 period.

• Projection of average monthly discharge and available volume through mathematical modeling, mainly from rainfall contributions and small springs present in the region. The resulting monthly average discharge values are shown in Table 5.

Table 5. Monthly average discharge record of the basin under study

Month	Average Q (l/s)
Jan	284.91
Feb	297.40
Mar	275.73
Apr	121.12
May	59.96
Jun	32.00
Jul	28.61
Aug	43.45
Sep	63.51
Oct	100.31
Nov	140.89
Dec	182.69

Souce: Technical Report No. 002-2020 ANA-AAA-CH.CH [21].

• Development of the monthly water availability predictive model in the Chalcas River Basin, using ANN of the MLP type. Also known as pattern mapping, it has the ability to learn to recognize and classify configurations through a supervised learning process. The elements it classifies are commonly vectors composed of binary values (0 and 1), and the resulting classes are also represented by binary vectors. This model consists of two levels of processing units (PUs), but only one of these layers has the ability to adjust the weights of its connections. Although the Perceptron architecture can incorporate additional layers, these do not have the ability to modify their connections without external intervention. The network was designed with three hidden layers (128, 64, and 32 neurons, respectively) and one output layer, using ReLU activation functions and a total of 11,265 trainable parameters. It was trained using the backpropagation algorithm, optimizing synaptic weights over multiple epochs to minimize prediction error. Model validation was carried out by calculating the RMSE and the statistical accuracy of the model, comparing observed and estimated values of monthly streamflow to verify the predictive capability of the generated model. The architecture of the MLP network is illustrated in Figure 1.

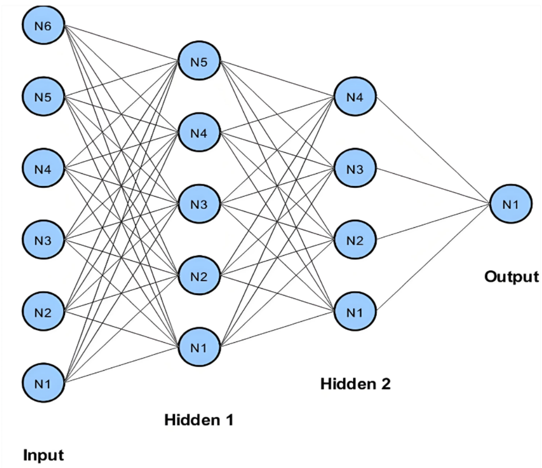

Figure 1. Multilayer neural network diagram

The dataset used included 276 monthly records corresponding to the period from January 1980 to December 2002. The input variables were: monthly precipitation (mm), average monthly temperature (°C), The complete architecture of the ANN is summarized in Table 6. ETo (mm), basin area (km^2), average slope (%), and drainage density (km/km^2). The output variable was the average monthly streamflow (l/s), considered a direct indicator of water availability.

Table 6. Architecture of the artificial neural network (ANN) used to estimate water availability

Layer	Layer Type	No. of Neurons	Activation Function	Trainable Parameters
Layer 1	Dense (input)	128	ReLU	896
Layer 2	Dense	64	ReLU	8256
Layer3	Dense	32	ReLU	2080
Output layer	Dense	1	Linear	33
Total	–	–	–	11,265

The process encompasses Preparation and Normalization (data organized and scaled between 0 and 1 using MinMaxScaler), Compilation and Training (the Adam optimizer, MSE loss function and MAE metric were used. Early Stopping was applied to avoid overfitting), Precision (achieved an accuracy of 89.11%, with a MAE of 0.0528 on normalized data), Prediction and Denormalization (the predictions were returned to their original scale to be compared with the actual values). Once trained, the model generates predictions based on the normalized data. 50 independent simulations were carried out in Google Colaboratory to verify the stability of the model under different random initializations. The selected architecture (128, 64, and 32 neurons) achieved an average accuracy of 90.62%, demonstrating high robustness, stability, and generalization capacity even with limited data. The full results of these 50 simulations are reported in Table 7.

Table 7. Result of 50 independent simulations of the artificial neural network (ANN) model to verify the stability of the training against different random initializations

Simulation	Accuracy (%)	Simulation	Accuracy (%)
1	91.51	26	90.27
2	89.89	27	90.98
3	91.16	28	91.05
4	91.23	29	90.38
5	89.74	30	89.93
6	91.58	31	91.41
7	91.57	32	90.48
8	91.29	33	90.01
9	91.57	34	91.13
10	90.48	35	91.56
11	90.37	36	90.52
12	89.63	37	90.66
13	91.28	38	90.12
14	89.9	39	91.25
15	90.17	40	90.13
16	90.4	41	91.77
17	90.93	42	90.29
18	91.03	43	90.8
19	90.78	44	91.46
20	89.83	45	91.18
21	90.99	46	90.95
22	88.88	47	89.53
23	87.82	48	91.3
24	90.22	49	90.11
25	90	50	91.42
Average accuracy	90.62		

3 Results and Discussion

The input variables included historical precipitation data (1980–2002), Kc, monthly ETo, water demand, and geomorphological characteristics of the basin. The model was trained in five independent simulations, incorporating controlled Gaussian noise to evaluate its stability and generalization capability.

The optimal architecture of the model consisted of three hidden layers (128, 64, and 32 neurons) with ReLU activation function, and an output layer with a linear activation function. After training, monthly water availability values were projected for the period 2003–2030.

The intervals and improvements in significance between simulations correspond to the fact that all variables were normalized to the range [0,1] using the MinMaxScaler function of Scikit-learn, to ensure better algorithm efficiency. The dataset was then split using the train_test_split() function into 80% for training (221 records) and 20% for validation (55 records). This expanded database guarantees robust model training and avoids statistical limitations.

The results obtained from the five simulations carried out on water availability in the Chalcas River basin for the period 2003–2030 are shown in Figure 2.

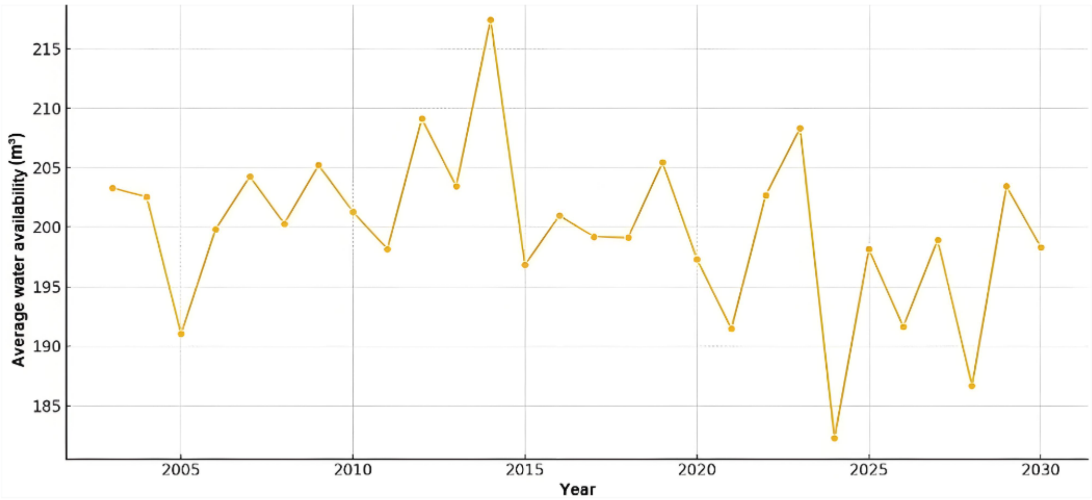

Figure 2. Annual average of water availability (2003–2030)

It represents the annual average water availability, allowing for the identification of years with higher or lower average resource supply. This visualization facilitates the detection of general trends over time, such as peaks of abundance or critical periods. The monthly distribution of average water availability is depicted in Figure 3.

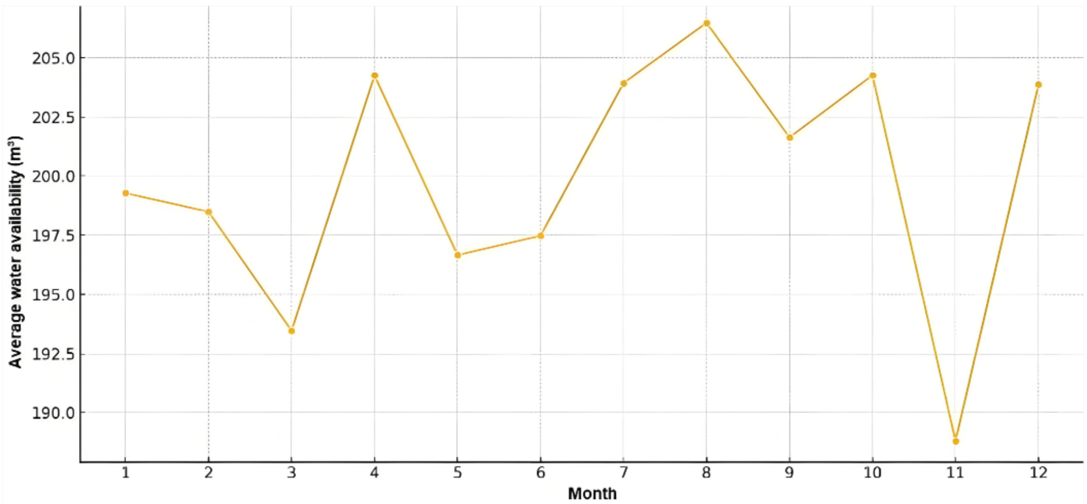

Figure 3. Monthly average of water availability (Average from 2003–2030)

The figure shows the accumulated monthly average over the simulated years, which allows recognition of seasonal patterns of higher or lower availability. Both representations support strategic water resource planning by highlighting annual and seasonal fluctuations that must be considered in integrated water management.

3.1 Projected Annual Trend (2003–2030)

The analysis of the annual average water availability showed values ranging between 190 m^3 and 218 m^3 per month. Years such as 2014 and 2023 were identified as having high availability, while 2024 and 2028 stood out for having the lowest figures, which may be related to simulated climate changes or interannual deficit accumulations. This information is essential for water resource planning, especially in agricultural contexts vulnerable to interannual variability.

3.2 Accumulated Monthly Average

The overall monthly average of water availability (accumulated 2003–2030) indicated that the months of April, August, October, and December had the highest values, exceeding 203 m^3/month. On the other hand, March and November were the most critical months, with averages close to 193 and 189 m^3/month, respectively. This seasonal pattern reveals the need to manage the resource differently throughout the year.

3.3 Variability Analysis

The variability of the projected data was assessed using the standard deviation and the coefficient of variation (CV). Months such as May and April were identified with high variability (CV $\approx$ 35%), suggesting greater model sensitivity to disturbances during these periods. In contrast, February and August showed lower variability, indicating more consistent predictions.

3.4 Seasonal Variation and Hydrological Behavior

The five simulations confirmed the existence of a consistent seasonal hydrological pattern. The months from January to March showed peak flows, with values exceeding 300 l/s (e.g., January 2027 with 305.96 l/s in Simulation 1). Conversely, the lowest values were recorded between June and August, ranging between 28–32 l/s. Hydrological recovery begins in September and consolidates in December with values close to 190 l/s.

3.5 Influential Climatological Factors

A strong correlation between seasonal precipitation and water availability was evident. The greatest water availability coincided with the rainy season (January–March), while scarcity was associated with the dry season (May–August), reinforced by the effect of ETo, where during the dry months (June–August), streamflow levels are low. This behavior is closely linked to temperature, which influences water loss from the system.

3.6 Practical Application of the Model

The model was designed to support water resource planning over a full projection horizon (2003–2028). Its main purpose is to identify critical and favorable periods, improving irrigation system management. Monthly forecasting allows for the anticipation of surpluses that can be stored or shortages requiring early interventions, reducing risks and optimizing water use.

3.7 Comparison with Previous Studies

The results of this study confirmed the robustness of the ANN model developed for predicting monthly water availability in the Chalcas River basin. Through five consecutive simulations, the model achieved an average accuracy of 90.62%, showing consistent and reliable behavior in estimating projected streamflows. Additionally, a low MAE was maintained across all runs, indicating a proper fit and generalization capacity. These outcomes highlight the ANN's ability to capture seasonal and interannual variations in water availability, exceeding expected performance for limited datasets. Compared with similar studies where error margins vary between 5% and 10%, the model developed here falls within an optimal accuracy range, validating its utility as a tool for sustainable water resource planning and management in rural and highly variable climate contexts.

However, as in other studies, model quality heavily depends on the availability and accuracy of input data. The lack of local hydrometric stations presents a significant challenge, suggesting the need to complement information with data from nearby stations or spatial interpolation techniques.

Based on the above, the application of ANN in this study has proven to be an effective tool for estimating water availability in the Chalcas River basin. Compared to previous research, ANN has been successfully applied in various hydrological contexts, from reservoir flow prediction to potable water demand management and hydrograph estimation in flood-prone basins. Nonetheless, to enhance the model's reliability in future research, it will be essential to strengthen data collection in the region and explore the integration of hybrid models combining traditional hydrological methods with artificial intelligence.

Castillo [23] implemented a model using data from multiple hydrological stations, achieving high accuracy with errors of less than 10%. While his focus was on reservoir management for hydroelectric power generation, his methodology—based on converting water levels into flow rates using a calibration curve—is similar to the procedure used in this study, where flow rate estimation is based on precipitation, ETo, and Kc [24].

In a context more focused on water demand, previous research used ANNs to predict water use patterns with meteorological variables such as temperature and precipitation, focusing on water supply rather than demand. Like the present research, they share the use of MLP as the core model architecture and statistical metrics for validation, reinforcing the reliability of this technique in various hydrological fields and demonstrating its viability [21].

A related study on the prediction of events such as floods, using ANNs. However, it does not address flood risk management. This research achieved the prediction of water availability, recommending that ANN models can be used both to optimize water distribution in agricultural systems and to improve water management in emergency situations [23].

3.8 Model Evaluation

The model achieved an average accuracy coefficient of 90.62% in the five simulations, with low MAE (<9.4%). This level of precision validates its reliability for medium-term monthly estimations, even with limited historical datasets. The observed performance is within the optimal range for ANN models applied in similar contexts.

4 Conclusions

The ANN-based predictive model developed in this study successfully met its primary objective, achieving an average accuracy of 90.62% and a normalized MAE of 0.0528. These results demonstrated the model's high capacity for estimating water availability in the Chalcas River basin with a low error margin, and its performance remained consistent across 50 independent simulations, confirming robust adaptation to seasonal and interannual flow variations.

Flow forecasting allows for the optimization of water distribution and use in the agricultural sector, an area with high water demand. It enables farmers and irrigation district managers to plan plantings and select the most suitable crops in advance, adjusting expected water needs to the forecasted water availability. Furthermore, it facilitates the efficient allocation of water by supporting the implementation of smart irrigation systems or precision agriculture, which adjust water delivery to the precise moment and amount, thus achieving efficient use of the resource. It also helps anticipate periods of scarcity or drought, allowing for the implementation of conservation measures, restrictions, or the search for alternative sources.

In civil and hydraulic engineering, flow predictions are essential for sizing and planning works that interact with water, guaranteeing their functionality and safety, such as the designs of dams, reservoirs, irrigation canals, aqueducts and storm sewers; it is crucial to know the maximum flows (to prevent failures due to flooding) and the minimum flows (to ensure supply).

The main limitations for this model are related to data quality, with the scarcity or inaccuracy of historical data; many models are based on long time series of flows and precipitation. Another limitation is the impact of uncontrolled external factors such as changes in the environment, land use and cover, as well as climate, which introduce increasing uncertainty in long-term predictions.

5 Recommendations

It is recommended to improve the ground-based monitoring network by increasing the quantity and quality of on-site gauging and meteorological stations, and modernizing them with real-time transmission technologies (IoT) for near-instantaneous data assimilation.

The widespread adoption of remote sensing represents a key strategy for overcoming data scarcity limitations and the inaccessibility of certain watersheds. This would involve using satellite data to estimate critical hydrological variables that are difficult to measure on-site, as well as monitoring water use with high-resolution satellite imagery to estimate actual ETo and irrigation water consumption, thus enabling better control of unregulated water withdrawals.

Author Contributions

Conceptualization, H.L.-A. and J.T.-V.; methodology, H.L.-A. and E.L.-P.; software, H.L.-A. and J.E.-C.; validation, H.L.-A., R.A.-B., and M.T.-P.; formal analysis, H.L.-A. and R.B.-A.; investigation, H.L.-A., J.T.-V., and A.I.; resources, H.L.-A.; data curation, H.L.-A. and E.L.-P.; writing—original draft preparation, H.L.-A.; writing—review and editing, J.T.-V., E.L.-P., and J.E.-C.; visualization, H.L.-A. and M.T.-P.; supervision, J.T.-V. All authors have read and agreed to the published version of the manuscript.

Data Availability

The data used to support the findings of this study are available from the corresponding author upon request.

Acknowledgements

Extend special recognition to the communities living in the Chalcas River basin for their ancestral bond with water and the land. The authors deeply value their respect for nature and connection to the territory and honor their ancestors, who have preserved practices that, today more than ever, inspire the authors toward sustainable water management.

Conflicts of Interest

The authors declare that they have no conflicts of interest.

References

[1] A. K. Biswas, “Integrated water resources management: A reassessment,” *Water Int.*, vol. 29, no. 2, pp. 248–256, 2004. https://doi.org/10.1080/02508060408691775

[2] S. B. Mirassou, “Integrated water resources management: Contributions to a conceptual development for water governance,” FLACSO, Argentine Academic Headquarters, Buenos Aires, 2009. http://hdl.handle.net/10469/1365

[3] J. C. Refsgaard and B. Storm, “Construction, calibration and validation of hydrological models,” in *Distributed Hydrological Modelling*. Kluwer Academic Publishers, 1996, pp. 41–54. https://doi.org/10.1007/978-94-009-0257-2_3

[4] L. S. Pereira, I. Cordery, and I. Iacovides, “Coping with water scarcity,” International Hydrological Programme. UNESCO-IHP, 2002. https://unesdoc.unesco.org/ark:/48223/pf0000127846

[5] V. T. Chow, D. R. Maidment, and L. W. Mays, *Applied Hydrology*. McGraw-Hill, 1988.

[6] W. Buytaert, R. Célleri, B. De Bièvre, F. Cisneros, G. Wyseure, J. Deckers, and R. Hofstede, “Human impact on the hydrology of the Andean páramos,” *Earth-Sci. Rev.*, vol. 79, no. 1-2, pp. 53–72, 2006. https://doi.org/10.1016/j.earscirev.2006.06.002

[7] W. Scharffenberg, M. Bartles, T. Brauer, M. Fleming, and G. Karlovits, “Hydrologic modeling system HEC-HMS: User’s manual,” US Army Corps of Engineers, Hydrologic Engineering Center, 2018. https://www.hec.usace.army.mil/software/hec-hms/

[8] K. W. Ng, Y. F. Huang, C. H. Koo, K. L. Chong, A. El-Shafie, and A. N. Ahmed, “A review of hybrid deep learning applications for streamflow forecasting,” *J. Hydrol.*, vol. 625, p. 130141, 2023. https://doi.org/10.1016/j.jhydrol.2023.130141

[9] V. P. Singh and D. A. Woolhiser, “Mathematical modeling of watershed hydrology,” *J. Hydrol. Eng.*, vol. 7, no. 4, pp. 270–292, 2002. https://doi.org/10.1061/(ASCE)1084-0699(2002)7:4(270)

[10] H. R. Maier and G. C. Dandy, “Neural networks for the prediction and forecasting of water resources variables: A review of modeling issues and applications,” *Environ. Model. Softw.*, vol. 15, no. 1, pp. 101–124, 2000. https://doi.org/10.1016/S1364-8152(99)00007-9

[11] H. Balacumaresan, M. A. Imteaz, and I. Hossain, “Superiority of artificial neural networks over conventional hydrological models in simulating urban catchment runoff,” *J. Hydroinformatics*, vol. 26, no. 9, pp. 2162–2186, 2024. https://doi.org/10.2166/hydro.2024.036

[12] W. A. Castaneda Sanchez, B. R. Polo Escobar, and F. Vega Huincho, “Artificial neural networks: A learning forecast measurement as potential demand,” *Univ., Cienc. Tecnol.*, vol. 27, no. 118, pp. 51–60, 2023. https://doi.org/10.47460/uct.v27i118.686

[13] H. Tamiru and M. O. Dinka, “Application of ANN and HEC-RAS model for flood inundation mapping in the lower Baro Akobo river basin, Ethiopia,” *J. Hydrol. Reg. Stud.*, vol. 36, p. 100855, 2021. https://doi.org/10.1016/j.ejrh.2021.100855

[14] M. B. Gunathilake, C. Karunanayake, A. S. Gunathilake, N. Marasingha, J. T. Samarasingue, and I. M. Bandara, “Hydrological models and artificial neural networks (ANNs) to simulate streamflow in a tropical catchment of Sri Lanka,” *Appl. Comput. Intell. Soft Comput.*, vol. 2021, no. 1, p. 6683389, 2021. https://doi.org/10.1155/2021/6683389

[15] K. Javan, M. R. Lialestani, and M. Nejadhossein, “A comparison of ANN and HSPF models for runoff simulation in Gharehsoo river watershed, Iran,” *Model. Earth Syst. Environ.*, vol. 1, no. 4, p. 41, 2015. https://doi.org/10.1007/s40808-015-0042-1

[16] I. N. Daliakopoulos and I. K. Tsanis, “Comparison of an artificial neural network and a conceptual rainfall–runoff model in the simulation of ephemeral streamflow,” *Hydrol. Sci. J.*, vol. 61, no. 15, pp. 2763–2774, 2016. https://doi.org/10.1080/02626667.2016.1154151

[17] P. Jimeno, J. Senent, J. Pérez, and D. Pulido, “A comparison of SWAT and ANN models for daily runoff

simulation in different climatic zones of peninsular Spain," *Water*, vol. 10, no. 2, p. 192, 2018. https://doi.org/10.3390/w10020192

[18] M. Ahooghalandari, M. Khiadani, and G. Kothapalli, "Assessment of artificial neural networks and IHACRES models for simulating streamflow in Marillana catchment in the Pilbara, Western Australia," *Aust. J. Water Resour.*, vol. 19, no. 2, pp. 116–126, 2015. https://doi.org/10.1080/13241583.2015.1116183

[19] V. K. Vidyarthi and A. Jain, "Does ANN really acquire the physics of the system? A study using conceptual components from an established water balance model," *J. Hydroinformatics*, vol. 25, no. 4, pp. 1380–1395, 2023. https://doi.org/10.2166/hydro.2023.025

[20] G. R. Humphrey, M. S. Gibbs, G. C. Dandy, and H. R. Maier, "A hybrid approach to monthly streamflow forecasting: Integrating hydrological model outputs into a Bayesian artificial neural network," *J. Hydrol.*, vol. 540, pp. 623–640, 2016. https://doi.org/10.1016/j.jhydrol.2016.06.026

[21] National Water Authority of Peru (ANA) and Municipality of San Pedro de Palco, "Technical report no. 002-2020 ANA-AAA-CH.CH-ALA GRANDE: Improvement of the Chalcas irrigation canal, San Pedro de Palco, Lucanas, Ayacucho," 2020. https://hdl.handle.net/20.500.12543/4734

[22] L. Ordoñez, S. Muñoz, P. Tineo, and I. Mejía, "Application of artificial neural networks to the modeling of rain-runoff in the Chancay Lambayeque river basin," *Tecnol. Cienc. Agua*, vol. 15, no. 6, pp. 95–141, 2024. https://doi.org/10.24850/j-tyca-2024-06-03

[23] J. Castillo, "Evaluation of forecasting models to estimate inflow to the Mazar reservoir: Application with neural networks," Master's thesis, Catholic University of Cuenca, Ecuador, 2023. https://dspace.ucacue.edu.ec/handle/ucacue/13892

[24] H. Gunathilake, V. Jayasooriya, A. Manathunge, and A. Pathirana, "Superiority of artificial neural networks over traditional hydrological models in flood prediction: Acomprehensive review," *J. Hydroinformatics*, vol. 26, no. 9, pp. 2162–2191, 2024. https://doi.org/10.2166/hydro.2024.036